

RESEARCH PAPER

## Synthesis of Ni Supported Mesoporous Carbon Nitride Nanocatalyst for Selective Hydrogenation of Acetylene to Ethylene

Fatemeh Dodangeh<sup>1</sup>, Alimorad Rashidi<sup>2\*</sup>, Hossein Aghaie<sup>1</sup>, Karim Zare<sup>1</sup>

<sup>1</sup> Department of Chemistry, Science and Research Branch, Islamic Azad University, Tehran, Iran

<sup>2</sup> Nanotechnology Research Center, Research Institute of Petroleum Industry (RIPI), Tehran, Iran

### ARTICLE INFO

#### Article History:

Received 18 April 2021

Accepted 24 June 2021

Published 01 July 2021

#### Keywords:

Acetylene

Ethylene

Hydrogenation

Mesoporous carbon nitride

Nanocatalyst

Polyol synthesis

### ABSTRACT

In this study, a nickel nanocatalyst was synthesized over a mesoporous carbon nitride (MCN), then used as catalyst support that was loaded by Ni nanoparticles for selective hydrogenation of acetylene in ethylene. The base of the catalyst was examined by the first polyol method with 15% by weight of nickel and the synthesized sample of the catalyst at temperatures of 700/800/900 was examined. Ni / MCN Catalysts Using methods FESEM, TPO, ICP, TGA, TEM, BET, FTIR, XRD, TPR, and Reactor tests were characterized. industrial catalyst Ni /  $\gamma$  Aluminum The catalytic performance of nanocatalysts was evaluated in the temperature range of 200-40 °C. New operating conditions for selective hydrogenation of acetylene in an ethylene-rich stream were introduced. As the temperature rises, it makes a very promising choice for ethylene production and also suppresses oligomer formation during acetylene hydrogenation. This nanocatalyst yielded significantly higher than 93% of what had previously been obtained for the production of ethylene was found that loading Ni on MCN led to a performance with about 99 acetylene conversion. performance compared to the G58C catalyst. Finally, acetylene and ethylene selectivity in different ratios of acetylene and hydrogen inlet feed in the hydrogenation reaction were investigated. In addition to increasing the temperature or decreasing the H<sub>2</sub> / AC molar ratio, the selectivity to ethylene is 96 compared to 78% conversion by commercial catalysts.

### How to cite this article

Dodangeh F, Rashidi A, Aghaie H, Zare K. Synthesis of Ni Supported Mesoporous Carbon Nitride Nanocatalyst for Selective Hydrogenation of Acetylene to Ethylene J Nanostruct, 2021; 11(3):432-445. DOI: 10.22052/JNS.2021.03.003

### INTRODUCTION

ethylene is industrially produced by the thermal or catalytic explosion of higher hydrocarbons. After the separation of the products, acetylene impurities are usually present in the ethylene-rich stream, which can poison traditional polymerization catalysts. Selective catalytic hydrogenation of acetylene is an important industrial process to eliminate the effects of acetylene in ethylene-rich flow to produce

polymer-grade ethylene. Commercially available Ni (nickel) based catalysts have their problems in this regard. In other words, they lead to poor ethylene selection in high acetylene conversion. [1-3]

In addition, they form an undesirable oligomer during acetylene hydrogenation. In addition, catalyst deactivation using coke deposition requires repeated catalyst regeneration processes used in the hydrogen reactor. Finally, these Ni-

\* Corresponding Author Email: [Rashidiam@ripi.ir](mailto:Rashidiam@ripi.ir)



based catalysts are highly temperature-sensitive. since the increase in temperature in the hydrogen production reactor, these types of commercial catalysts lose more choice than ethylene, therefore, more ethylene is consumed, so the temperature rises again. A common behavior of current catalysts is to reduce the choice of ethylene due to acetylene conversion or increase in temperature.[4]

So the temperature rises again. A common behavior of current catalysts is to reduce the choice of ethylene due to acetylene conversion or increase in temperature. Therefore, in practice, two reactors with cooling operations are usually used to completely remove acetylene impurities during the ethylene feeding process, which are referred to as tail-end processes.[1-8]

Fig. 1 shows that the acetylene hydrogenation reaction pathway is a better pathway for ethylene production. Other pathways lead to by-products and the formation of green oil. [14] The base of the catalyst is an influential parameter in the hydrogenation reaction. This is because of the fact that the support can change the absorption power of the catalyst and as a result, they can regulate the choice of ethylene. The basic surface is an important factor in the activity of the catalyst [9-10] and any size The higher the surface area and the volume of the cavities, the higher the percentage of metal that can be placed on the base [11].

The base porosity also controls the particle size of the catalyst. Catalyst support includes metal oxides such as  $\text{TiO}_2$ ,  $\text{Al}_2\text{O}_3$ , or  $\text{SiO}_2$ , carbon structures such as graphene or CNT, metal carbides, zeolites, and more. Based on the extreme importance of the catalyst base in this selective reaction [12-14], Huang et al. [13] have shown that although Ni-filled graphene produces higher activity, Ni-filled carbon nitride due to its very high acidity and porosity. Leads to better selectivity of ethylene. Carbon nitride (CN) is an attractive material with unique properties such as semiconductor, base, high hardness, chemical resistance, and high chemical and mechanical stability. Nitrogen mixing in CN carbon matrices not only provides a unique electronic structure with a bandgap of less than 2.7 eV, but also helps to enhance field emission, photocatalysis, and carbon capture, and energy storage. The properties of CN materials are mainly controlled by the structure, composition, and crystallization of the CN framework. [14-17]

Mesoporous carbon nitrides (MCN) are unique semiconductor materials with wide surface area and uniform pore diameters and have very diverse and excellent physical and chemical properties in various fields such as catalyst base, energy storage and conversion, hydrogenation, Absorption, separation, and even gas sensing are used. These attractive MCN materials can be obtained by polymerization of various aromatic and/or aliphatic carbons and molecular precursors containing high nitrogen through hard methods and/or soft experiments. MCNs have a high ability to absorb metals due to their high porosity level. The combination of MCN with metal nanoparticles such as Pd, Pt, Ni shows excellent properties in hydrogenation and adsorption of acetylene gas and its conversion to ethylene. We examine the potential of these materials by reviewing key and relevant results. Special emphasis is also placed on the catalytic applications of MCNs, including the hydrogenation of acetylene to ethylene and the activation of  $\text{CO}_2$ . Various methods are available for the synthesis of CNs, including thermal decomposition or polymerization of nitrogen-containing molecules such as melamine, urea, thiourea, cyanamide (CA), and so on. Recently, peeling pathways have also been successfully developed to produce a nanogram sheet of a gram. But Zhao et al reported the synthesis of very regular MCNs with very high levels using the same HMT as precursors C and N and SBA-15 as a hard pattern in the nano-casting process. This was attributed to the complete cross-linking of precursors C and N and the massive release of nitrogen, leaving a large amount of fine porosity in the CN walls at high temperatures. It is also assumed that the difference in gas production temperature and the ratio of SBA-15 and HMT make a large difference in the final properties of MCN [18].

In another work [12], it has been reported that high back acidity can improve coke resistance as well as Pd catalyst selection. Huang et al. [14] showed by comparing the selectivity of ethylene in Pd-filled graphite carbon nitride support ( $g\text{-C}_3\text{N}_4$ ) to different catalyst supports such as  $\text{SiO}_2$ ,  $\text{Al}_2\text{O}_3$ , etc. that carbon nitride support can be compared with  $\text{Al}_2\text{O}_3$  and  $\text{SiO}_2$  significantly improves the selectivity of ethylene. In addition, the resistance to coke formation has been improved. Therefore, it is obvious that the support of the catalyst as well as the modifiers must be carefully considered

to produce a highly active and selective catalyst. From the industrial point of view, green oil, which is an accumulation of polymer species, is the main problem in the process of acetylene hydrogenation. [19-20] According to the theory of Brodzinski et al. [21] Isolated sites can increase the selectivity to ethylene and thus increase the catalyst stability. Minimizes catalyst stability and paves the way for the development of new nanocatalysts with advanced performance in selective acetylene hydrogenation. Also, it has been suggested by Al Ammar et al. [16] that an isolated decomposition species that may be easily removed by hydrogen treatment at ambient temperature can act as a hydrogen transfer medium.[15]

According to their proposal, hydrogenation involves the transfer of hydrogen between a decomposed adsorption species and mass adsorption acetylene, rather than directly adding hydrogen to the adsorbed acetylene. In this regard, Podkolzin et al. [15] theoretically confirmed this mechanism of hydrogen transport by calculating the theory of density function (DFT). The results of their modeling indicate that there are three main effects of hydrocarbon coating on selection in ethylene production. First, they suggested that at high carbon coatings, ethylene desorption from hydrogenation becomes more competitive because the presence of spectator species destabilizes reactive species. They then presented the effect of activity changes due to unequal destabilization of reactive hydrocarbon species.[6]

In the present work, a new and selective nanocatalyst was synthesized by loading modified Ni particles on graphite carbon nitride supports. This work is the first attempt at doping the Ni nanoparticles over the carbon nitride with a high surface and effect of increasing temperature and decreasing H<sub>2</sub> / C<sub>2</sub> ratio for performance in ethylene selectivity.

## MATERIALS AND METHODS

### Synthesis of SBA15

According to Zhao et al. [20], SBA-15 was first synthesized as an MCN model. Briefly, p123 (pluronic acid) was dissolved in a mixture of DI water and HCl solution. After that, TEOS (tetraethyl orthosilicate) solution prepared on a magnetic stirrer was added, the mixture was placed at 80 ° C overnight in the laboratory, and after washing, it was dried at room temperature in a nitrogen furnace at room temperature. 500 ° C was performed for 6 hours.

### Synthesis of MCN

A Mesoporous carbon nitride catalyst base was prepared by adding SBA-15 to a mixture of ethylenediamine, and carbon tetrachloride under magnetic stirring at 90 ° C for 6 hours. The resulting mixture was then dried for 12 hours and then placed in a furnace under nitrogen at 700, 800, and 900 ° C for 5 hours. To remove SBA-15 silicate plates, sample with 5% HF by the weight smoothed and then After filtering, washing with ethanol, and drying at 100 ° C, the MCN catalyst base was obtained.[18]

### Synthesis of MCN loaded with Ni

Metal-filled MCN was synthesized by adding 0.5 g of MCN to about 100 ml of mono ethylene glycol for 4 hours at 60 ° C with an ultrasonic device. Then, Ni (NO<sub>3</sub>)<sub>3</sub>·6H<sub>2</sub>O about 0.1% by weight (0.0008 g) was added to the resulting mixture and stirred for 12 h. In this method, ethylene glycol not only acts as a solvent but also has a reducing agent. Then, to intensify the reduction of Ni salt in ethylene glycol, the pH of the solution was adjusted to 11 using sodium hydroxide. In the next step, the result was refluxed at 90 ° C under N<sub>2</sub> gas for 6 hours, followed by filtration, washing with DI water, and drying at 80 ° C under N<sub>2</sub> gas for 4 hours. (Fig 2)

### Characterization

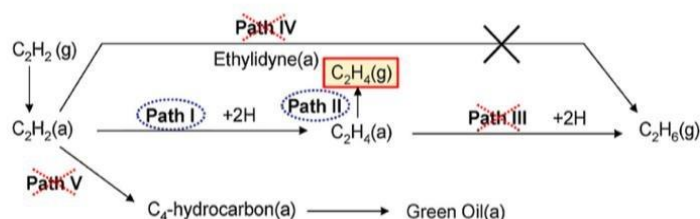


Fig. 1. Different pathways of acetylene hydrogenation reaction in the presence of ethylene [14].

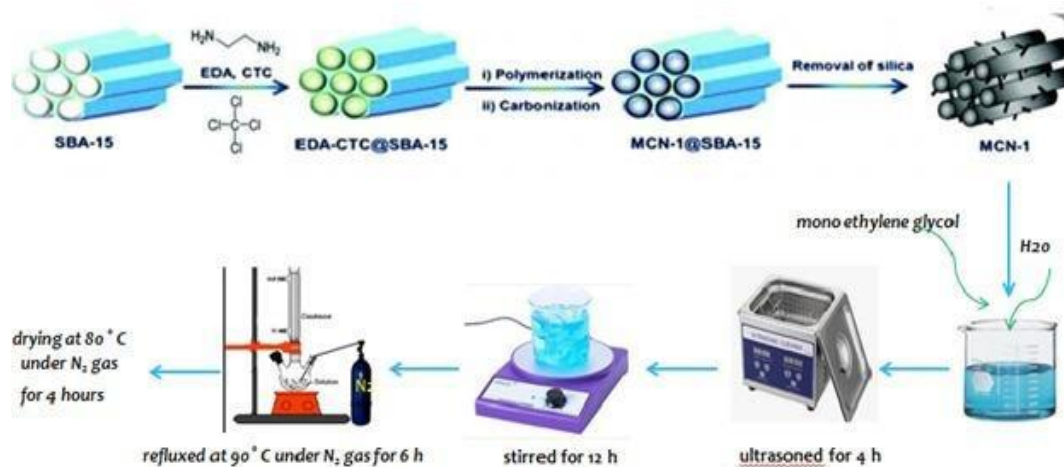


Fig. 2. Schematic synthesis of (MCN) and (MCN) doped with nickel.

### Physical Chemistry Properties of Catalysts

to characterize the catalyst support and also the nanocatalysts, Field Emission Scanning Electron Microscopy (FESEM) (TESCAN, model MIRA III), Transmission Electron Microscopy (TEM) (Philips, CM120), X-ray Diffraction (XRD) (Bruker AXS -D8 Advance), Nitrogen Adsorption/Desorption (Belsorp mini, Japan), Raman shift (TakRam N1-541) BET physical adsorption analysis was performed on the samples using a 2000-ASAP device, atomic emission method (I.C.P)( Varian VISTA-MPX), The thermal analyzer(TGA)(Perkin-Elmer TGA-7), Temperature Reduction Analysis(TPR) (Micromeritics TPD-TRP 2900), Temperature programmed oxidation(TPO),(Micromeritics TPD-2900 apparatus connected to a Pfeiffer Vacuum-300 mass spectrometer) and Fourier Transform Infrared (FTIR) (Thermo, AVATAR) Spectroscopy was employed.

### Reactor testing of samples

The catalytic performance of the nanocatalysts was evaluated in a stainless steel reactor with an internal diameter of 0.75 inches and a length of 60

cm. Reactions were performed in the temperature range of 40 to 200 ° C using a 0.1 g catalyst (size 2-4 mm) with 0.3 g of inert chromosome particles. Feed gas contained 88% ethylene, 10 mol% ethane, 1.4 mol% acetylene and, 0.8 mol% hydrogens. The feed rate was 40 cc per minute and the GHSV gas hourly rate was (33,000) hours per hour. The exhaust gas was analyzed by Varian 3800 gas chromatography with an FID detector. The performance of nanocatalysts was evaluated for acetylene conversion and ethylene selection, as well as green oil extracted from the reactor. The hydrogenation reactor is also shown in Fig.3.

### RESULTS AND DISCUSSION

#### Analysis quantification of quantitative elements of I.C.P.

The results of the I.C.P test are shown by the polyol method in Table 1, and as we can see, more than 98% of the predicted material is on the base.

#### Raman spectra analysis results

The Raman spectra of MCN samples are shown in Fig.4. For all specimens, corresponding to sp<sup>2</sup>-

Table 1. Results of I.C.P Nickel load analysis.

Catalyst name	Load percentage	Percentage of Nickel in the sample
Ni-MCN	15	14.85



Fig. 3. Experimental setup and reactor for acetylene and ethylene selectivity.

based irregular carbon and graphite, respectively, two distinct peaks appeared at about 1354 and 1570  $\text{cm}^{-1}$ . For the sample prepared at 700, 800, and 900 °C, ID / IG values of 1.81, 1.01, and 0.69 were obtained, respectively. From Raman's results it can be inferred that with increasing temperature, the degree of graphitization (G-band) of MCN samples has increased, which may lead to the destruction of the MCN structure.

*TGA level measurement results*

TGA analysis of MCN samples synthesized at different synthesis temperatures shows that it lost

only 5% of its weight from ambient temperature to about 370 °C due to the presence of carbon dioxide and impurities in the samples [18, 17]. Therefore, the stability of the catalyst, especially the stability of the base and its morphological preservation at high temperatures, of particular importance. According to Fig. 5. the synthesized catalysts are stable up to 300 °C. Since the hydrogenation reaction range is between 80-220 °C, thermal degradation does not effect our reaction. Thermal degradation at high temperatures is due to the breaking of the carbon-nitrogen bond.

*BET level measurement results*

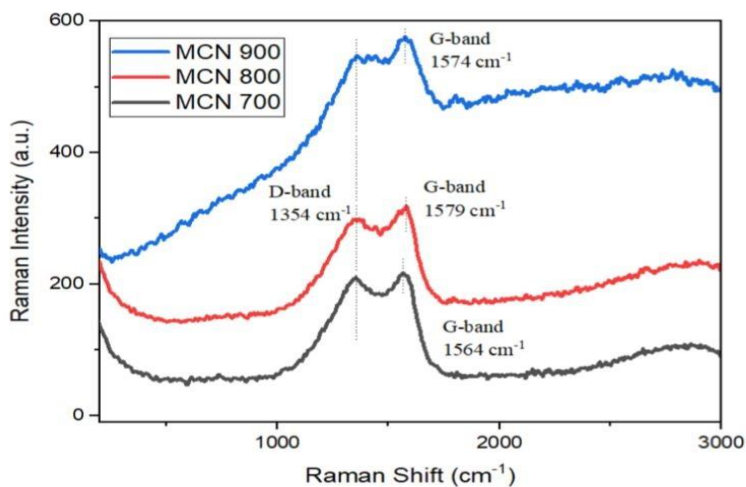


Fig. 4. Results of Raman analysis for MCN synthesized at temperatures of 700-800-900 °C.



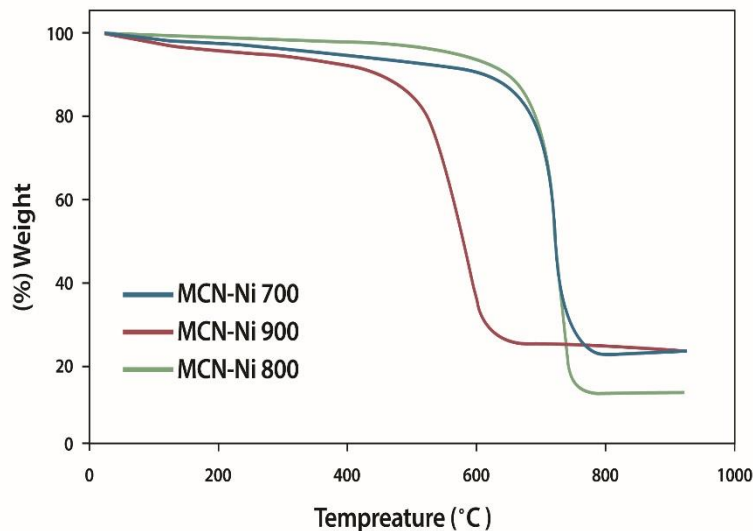


Fig. 5. TGA analysis of prepared sample at 700-800-900°C temperatures.

As can be seen, SBA-15 had a high SBET which decreased in MCN as well as Ni / MCN samples. The decrease in SBET in the Ni / MCN sample compared to MCN is attributed to the blockage of some pores, which is also evident in the reduction in the total pore volume. The higher the nickel loading percentage, the higher the selectivity of nickel. The large mesopores are effective in loading metals and active sites that the formation of undesirable products and green oil due to the reaction inside the cavities, which causes the canal to be deactivated. Also, The specific surface of the commercial catalyst was 40 m<sup>2</sup>/g along with a mean pore diameter of 30 nm.

**FESEM analysis results**

The FESEM images of the MCN catalyst support provided at 700 °C are shown in Fig. 6. As can be seen, the morphology of MCN was curved shells. According to previous researches on MCN synthesis and analysis, the synthesis has been done correctly.

**Results of TEM diffraction technique**

TEM images of MCN uploaded by active sites are shown in Fig. 7. In this figure, it is clear that Ni nanoparticles are loaded on the MCN. Particles accumulate inside the graphite lattice more than outside the lattice. In the case of the Ni / MCN sample, the TEM micrograph shows that the maximum Ni nanoparticles were 5-11 nm in size. For this example, the homogeneous distribution of active metal sites can be detected, which can be effective in the hydrogenation reaction of acetylene, while providing sufficient active sites and preventing the adsorption of excess reactants, thereby increasing the choice of ethylene.

**XRD X-ray diffraction technique analysis results**

XRD patterns of SBA-15, MCN, and MCN-Ni prepared nanocatalysts are shown in Fig. 8. According to SBA-15, a broad peak at 2θ was observed at about 23°. This peak is referred to as the SBA-15 precursor amorphous silica walls. [40] The XRD logo of the sample loaded with

Table 2 . Results from BET analysis.

Sample catalyst	Surface area (m <sup>2</sup> /g)	Total pore volume (cm <sup>3</sup> )	Average pore diameter (nm)
SBA-15	384	0.541	5.9
MCN	152	0.206	6.7
MCN-Ni	89	0.172	9.8

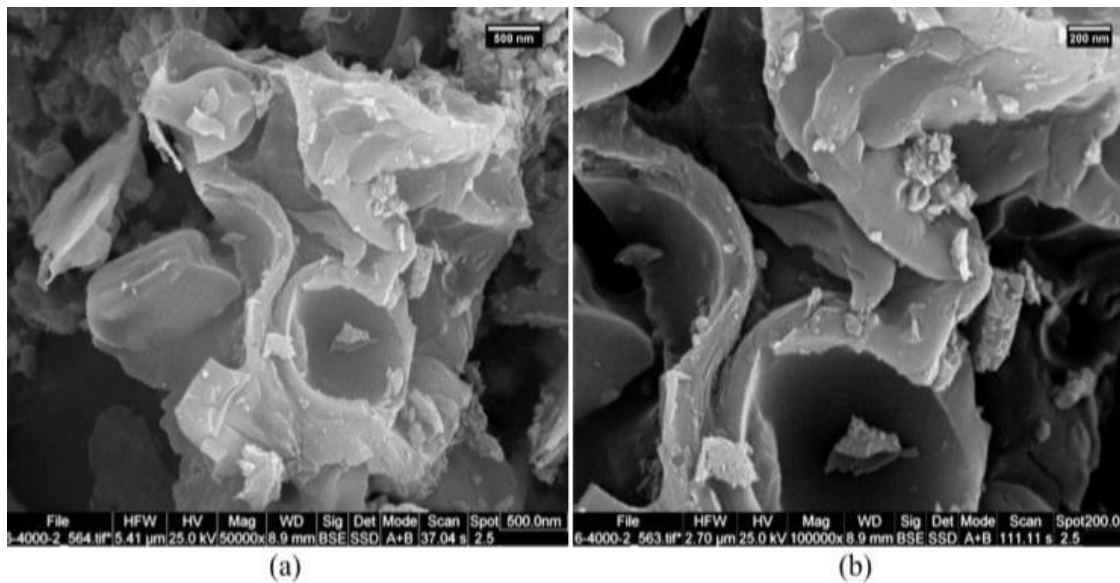


Fig. 6. The FESEM images of the prepared MCN catalyst support in 700 °C.

Ni was similar to the MCN base, except that it is a negligible peak at approximately 31e. This originates from Ni nanoparticles [19], however, because Ni nanoparticles are distributed on a small scale without any aggregation, no definite peaks have been observed. From the XRD results, it can be stated that Ni can be well distributed through MCN support and there is no sign of accumulation. XRD analysis of these 3 samples shows that MCN and SBA15 did not undergo structural disruption after metal adsorption.

*TPR analysis results*

The TPR results of Ni-MCN nanocatalyst are shown in Fig.9. The main peak in 300.4 is divided into three distinct peaks. Other peaks are related to impurities. The amount of hydrogen used to reduce nickel species, in theory, is 10.3 micromoles H<sub>2</sub> / g. Using the level below the peak, a diagram of 0.07 mmol has been obtained. The difference between these two values is related to the partial reduction of nickel-metal during synthesis by the poly method. The presence of nickel species has

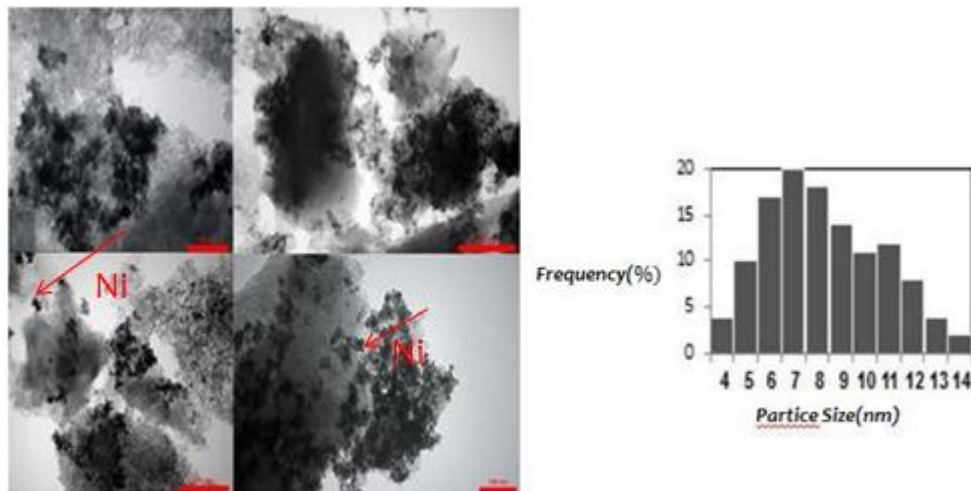


Fig. 7. Results from TEM analysis of Ni-MCN Nano catalyst.

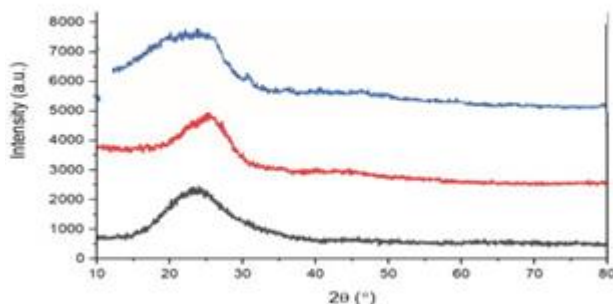


Fig. 8. A Result from XRD analysis of SBA-15, MCN samples and MCN-Ni .

also been observed in the XRD analysis. A peak at 45° related to metal impurities was reported in the sample.

*Results of catalyst performance test in fixed bed reactor*

*Hydrogenation of selective acetylene Ni / MCN and commercial catalyst*

The catalytic performance of Ni / MCN nanocatalysts in selective hydrogenation of acetylene was used and compared with commercial catalysts. The catalytic performance of Ni / MCN and commercial catalysts in terms of acetylene conversion and ethylene selection is shown in Fig. 10. Due to the conversion of acetylene, similar behavior has been recorded for both catalysts, and with increasing temperature, the conversion

of acetylene to ethylene has been continuously performed and increased. This is due to the higher hydrogenation activity of the catalysts at higher temperatures and faster reaction motion.

However, Ni / MCN showed much better performance at all temperatures, eventually reaching 96% compared to 78% conversion by commercial catalysts. This can be attributed to the effect of catalyst support in creating an improved distribution of active sites that are more present in the hydrogenation of acetylene molecules. The higher porosity and MCN level compared to the commercial G58C catalyst lead to much better acetylene conversion performance. In addition, the selection of ethylene in the catalyst follows the same trend, and with increasing temperature, the selection power increases, and after reaching

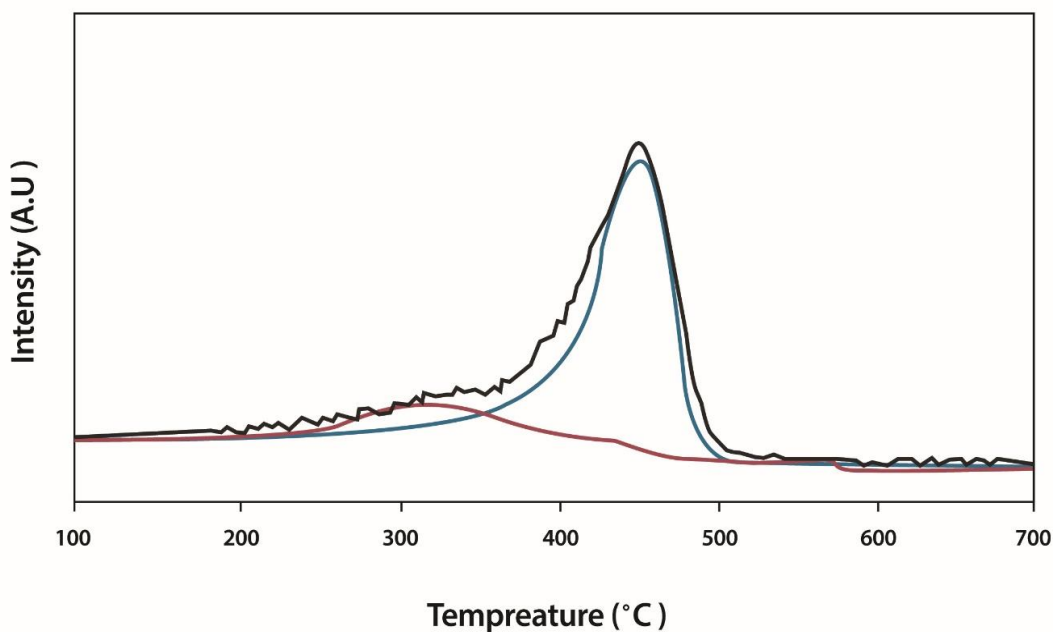


Fig. 9. TPR results of Ni-MCN nanocatalyst.



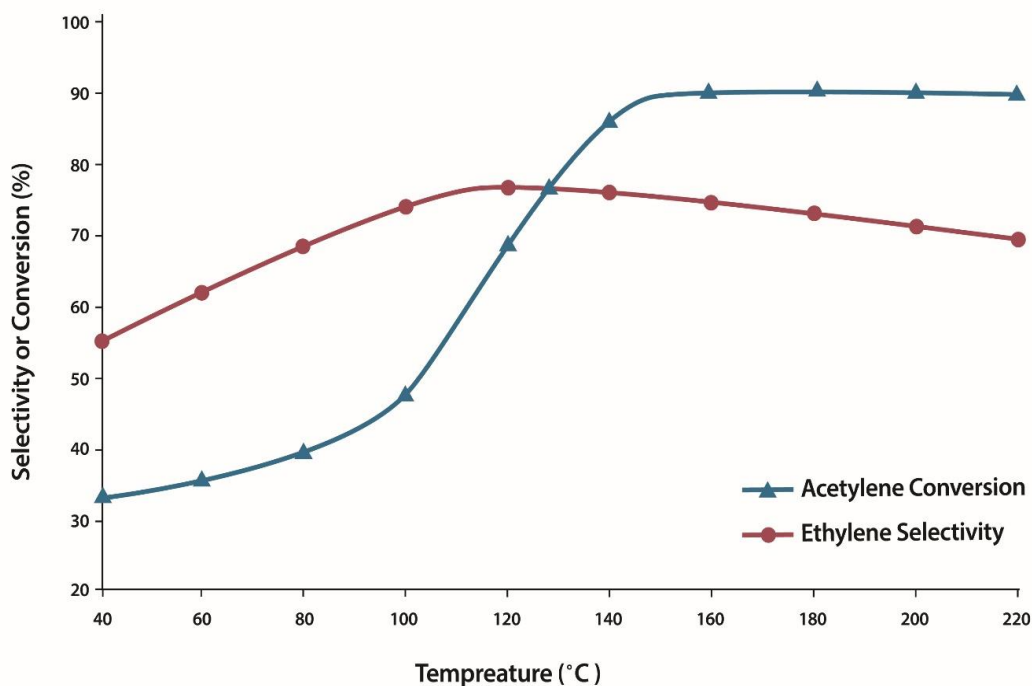


Fig. 10. The acetylene conversion and ethylene selectivity of the Ni/MCN and the commercial catalyst at 40-220

the desired temperature, the increase in ethylene selection decreases. The maximum selection of ethylene Ni / MCN and the commercial catalyst was obtained 120 times 83% and 72%, respectively. The selectivity of Ni-MCN catalysts is due to the formation of large mesopores at the base and the formation of ethylidyne, which eliminates the possibility of reactive access to the four coordination sites by occupying some nickel sites.

This is consistent with the literature focusing on the better performance of carbon nitride as support for Ni catalysts in the selective hydrogenation of acetylene.

Also, due to the high price of palladium and platinum metals in foreign catalysts, nickel can be used in the catalyst. "In this process, nickel replaces the precious metals palladium, platinum in catalyst manufacturing processes, which reduces the cost in this sector to sixteen.

#### Comparison of hydrogenation of selectivity of acetylene and selectivity of ethylene in Ni / MCN at different temperatures of MCN synthesis

Selective acetylene hydrogenation in nanocatalysts synthesized at different temperatures is shown in Fig. 11. all nanocatalysts

have resulted in an excellent acetylene conversion performance, therefore, the highest point in the diagram of these nanocatalysts is the highest selectivity of ethylene, by which the final performance of nanocatalysts can be evaluated. Ethylene is a dedicated nanocatalyst containing Ni, reducing the adsorption capacity of Ni sites to ethylene and preventing excessive hydrogenation of ethylene is essential According to Fig.11, increasing the temperature can improve the selectivity of ethylene, and finally, the selection of ethylene was 94.6% at 200 ° C, 96%. At low temperatures, the reaction products include ethylene, ethane, butene isomers, 1-3 butadiene, and a small amount of butane and the amount of green oil was negligible, while from about 160 ° C and above the amount number of by-products increased, followed by increased green oil production.

#### Comparison Results of Fresh Ni-MCN Nanocatalysts and Ni-MCN Nanocatalysts Used by TPO Analysis

Temperature-programmed oxidation (TPO) of the nanocatalyst used in this study showed that very little coke was deposited on this material (Fig. 14). Finally, it was confirmed that no adverse

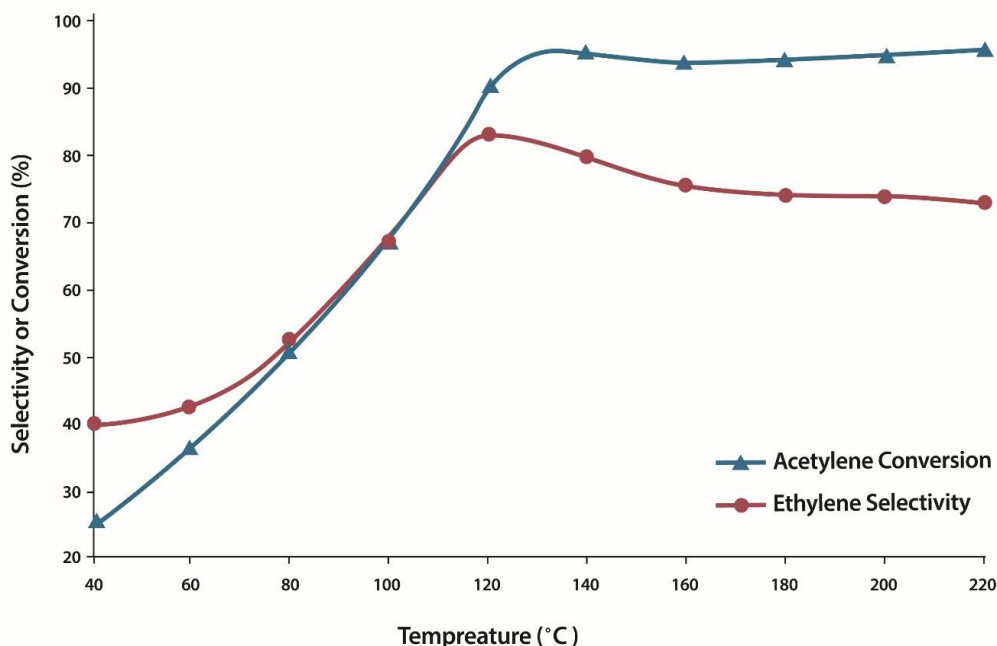


Fig. 11. Comparison of hydrogenation of acetylene conversion and selectivity of ethylene in Ni / MCN at different temperatures of MCN synthesis.

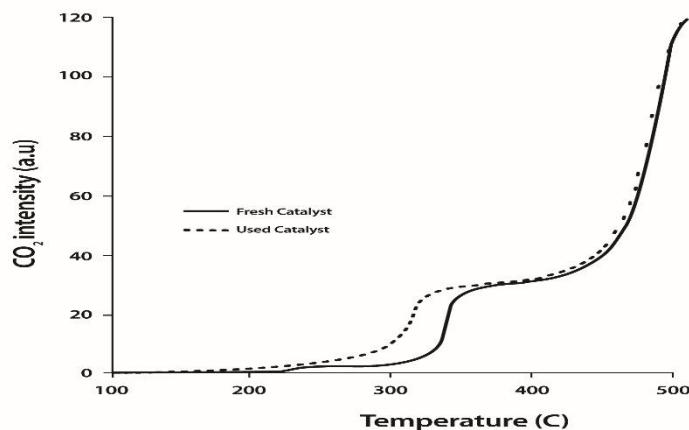


Fig. 12. TPO analysis results for used and fresh catalysts at different temperatures

reaction for oligomer formation of coke deposition in the nanocatalyst studied in This did not happen. In Fig. 12, the small amount of CO<sub>2</sub> detected at low temperatures may indicate the adsorption of carbon species on the catalyst.

*Results of selectivity of ethylene with different ratios of hydrogen to acetylene in Ni-MCN nanocatalyst*

Catalytic experiments were performed to study

selective activity and performance on a 50-hour stabilized sample under the proposed reaction conditions. In these experiments, gaseous mixtures of H<sub>2</sub> / C<sub>2</sub>H<sub>2</sub> molar ratios of 1, 1.2, and 1.3 with a total flow rate of 135 ml/min were passed through the catalyst bed as reactor feed and the product gases by GC. Was analyzed at the reaction temperature in the range of 220-80. In addition, at each test point, the temperature was maintained for 15 minutes to stabilize before analyzing the

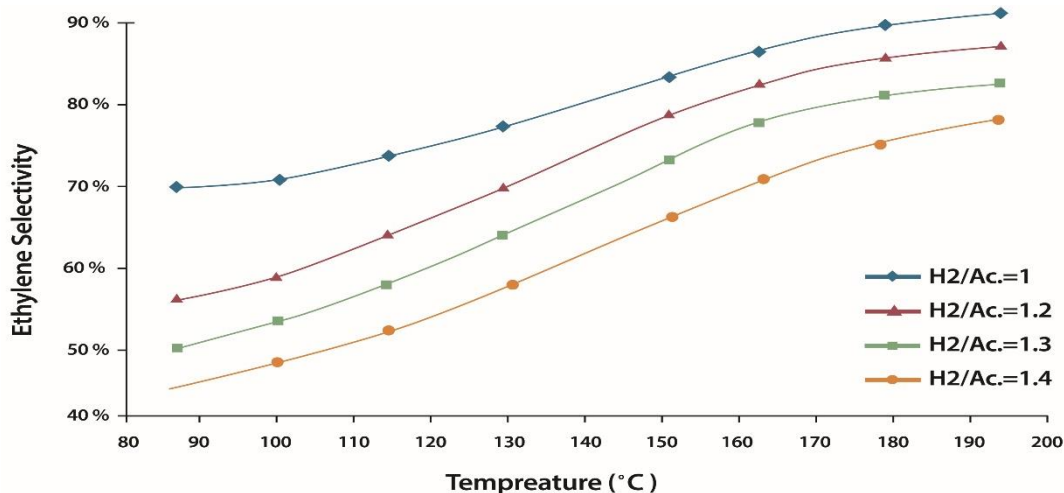


Fig. 13. Results of ethylene selectivity with different ratios of acetylene and hydrogen input feed

product.

These figures showed that for Ni / MCN catalysts, ethylene selection increases with both temperature and acetylene conversion. In other words, with increasing temperature, acetylene conversion and ethylene selection increased. These results were, on the one hand, in contrast to the selective behavior observed by many of the hydrogenation catalysts previously reported in the literature [42–37], while on the other hand, they supported several previous rather specific studies.

[46–43]

*Results of comparing ethylene selectivity and acetylene selectivity with different feed input ratios of acetylene and hydrogen*

According to Fig. 14, the amount of acetylene and the hydrogenation of ethylene both increase with temperature, the rate of ethylene desorption increases faster than the hydrogenation of ethylene with temperature. Increasing the surface area of acetylene with temperature was observed as

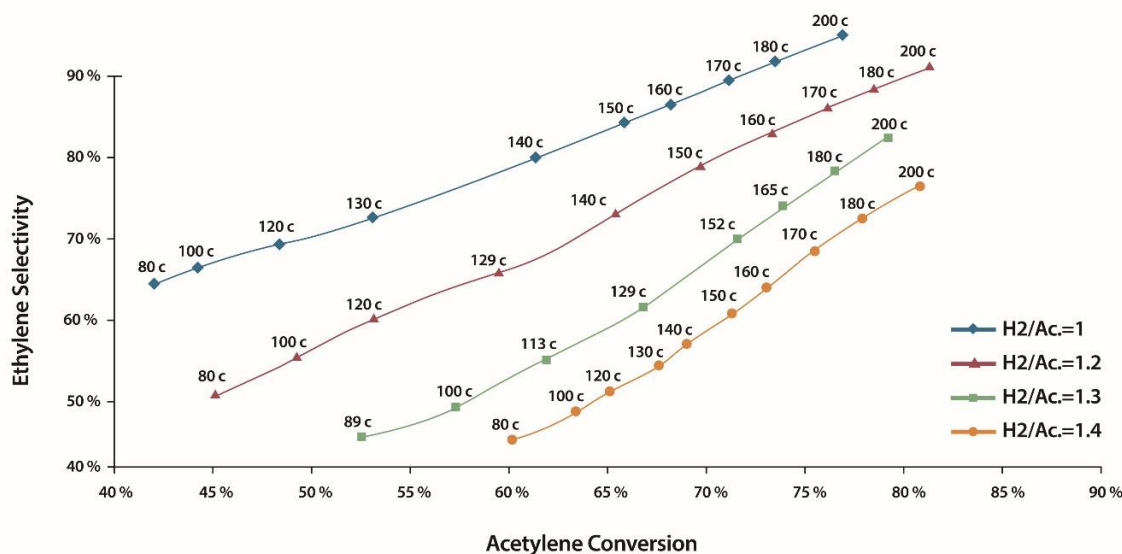


Fig. 13. Results of ethylene selectivity with different ratios of acetylene and hydrogen input feed

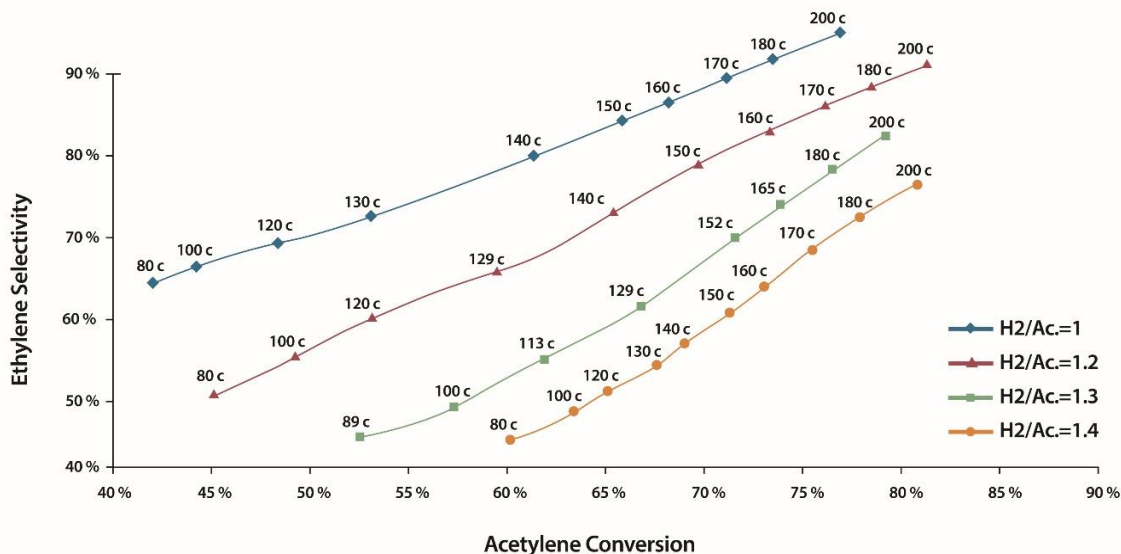


Fig. 14. Results of ethylene selectivity and acetylene selectivity with different ratios of acetylene and hydrogen input feed.

another complementary reason for increasing the choice of ethylene with temperature. Therefore, during the hydrogenation of acetylene through a catalyst, adverse reactions (e.g., mainly oligomer formation) do not occur or are suppressed by catalytic performance, the choice of ethylene is improved by temperature.

The formation of a thin layer of carbon on the Ni / MCN catalyst seriously affects the catalytic performance. Evidence, on the other hand. The following is a summary of the results obtained in this study to rationalize the mechanism governing acetylene hydrogenation on a synthesized Ni / MCN catalyst hydrogen transfer mechanism:

By increasing the H<sub>2</sub> / C<sub>2</sub> molar ratio to a critical value and beyond, the catalyst completely lost its choice over ethylene. This means that a significant change in the hydrogenation mechanism occurred in Ni / MCN due to the clearance of carbon deposits from the catalyst surface.

By increasing the temperature or decreasing

the H<sub>2</sub> / AC molar ratio, the selectivity to ethylene improves. These changes lead to the formation of more carbon species on the catalyst

Finally, the conversion of acetylene, as well as the choice of ethylene, increases with increasing temperature, which means that when undesirable side reactions are suppressed on the Ni / MCN catalyst, the hydrogen transfer mechanism is dominant. Therefore, with increasing temperature, activity increases Fig. 14. confirms the above results. This indicates that the choice of ethylene decreases while the conversion of acetylene increases at constant temperatures.

This figure highlights the essential role of the hydrogen transfer mechanism in the hydrogenation of acetylene on the Ni / MCN catalyst. In addition, he stressed that this mechanism is dominant as a governing factor when the temperature rises. It is noteworthy that, in previous studies, it was shown that due to the occurrence of hydrogenation reactions in series, at constant temperature

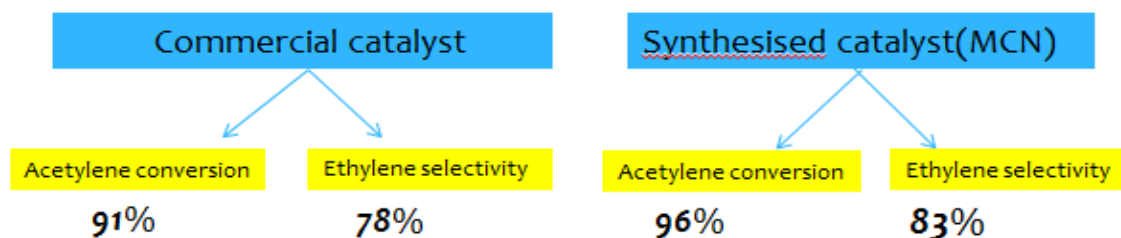


Fig. 15. Compare of acetylene conversion and Ethylene selectivity in commercial and synthesis catalyst (MCN)

ethylene selection decreases.

In addition, by increasing the conversion of acetylene, as a result of increasing the deposition of carbon species and the dominant hydrogen transfer mechanism of the nanocatalyst, increasing the temperature weakens the progression of these series reactions.

Finally, we show the conversion of acetylene and the selectivity of ethylene in commercial and synthesized catalysts in Fig. 15.

## CONCLUSION

In this research, a selective hydrogenation novel catalyst, as well as new process conditions for selective hydrogenation of acetylene in an ethylene-rich stream, were obtained and discussed. The nanocatalyst prepared at high temperature is so satisfactory that it is possible to remove acetylene impurities in ethylene feed in a single hydrogenation reactor.

Another result is that only a small amount of hydrogen enters the feed in a reactor using this catalyst. Finally, a very significant advantage of the present catalyst was its high performance for ethylene production, which reached a maximum of 96%.

High ethylene yield, as well as suppression of oligomer formation and greater stability than inactivation during selective hydrogenation of acetylene impurities in an ethylene-rich stream, make the Ni-MCN catalyst a future candidate for a successful selective hydrogenation selective catalyst for ethylene streams. Rich in acetylene, will convert in the future.

In this report, the optimum Ni nanoparticles distributed inactive sites over the MCN which possessed a high surface and total pore volume which was confirmed in the TEM images and the XRD patterns of nanocatalysts.

In addition, based on the results obtained in this work and comparisons with other data in the sources, the hydrogenation of acetylene on the Ni / MCN catalyst was rationalized to be done through the hydrogen transfer mechanism.

The synthesized sample could provide 96acetylene conversion and the ethylene selectivity of 83 which is an excellent performance.

## CONFLICT OF INTEREST

The authors declare that there are no conflicts of interest regarding the publication of this manuscript.

## REFERENCES

1. Hosseini SM, Ghiaci M, Farrokhpour H. Mechanistic Insight into the Hydrogenation of Acetylene on the Pd<sub>2</sub>/g-C<sub>3</sub>N<sub>4</sub> Catalyst: Effect of Pd Clustering on the Barrier Energy and Selectivity. Research Square Platform LLC; 2021.
2. Zhao Y, Zhu M, Kang L. The DFT Study of Single-Atom Pd1/g-C<sub>3</sub>N<sub>4</sub> Catalyst for Selective Acetylene Hydrogenation Reaction. Catalysis Letters. 2018;148(10):2992-3002.
3. Huang W, McCormick J, Lobo R, Chen J. Selective hydrogenation of acetylene in the presence of ethylene on zeolite-supported bimetallic catalysts. Journal of Catalysis. 2007;246(1):40-51.
4. Mei D, Neurock M, Smith CM. Hydrogenation of acetylene–ethylene mixtures over Pd and Pd–Ag alloys: First-principles-based kinetic Monte Carlo simulations. Journal of Catalysis. 2009;268(2):181-195.
5. Pei GX, Liu XY, Wang A, Lee AF, Isaacs MA, Li L, et al. Ag Alloyed Pd Single-Atom Catalysts for Efficient Selective Hydrogenation of Acetylene to Ethylene in Excess Ethylene. ACS Catalysis. 2015;5(6):3717-3725.
6. Zhou S, Shang L, Zhao Y, Shi R, Waterhouse GIN, Huang YC, et al. Pd Single-Atom Catalysts on Nitrogen-Doped Graphene for the Highly Selective Photothermal Hydrogenation of Acetylene to Ethylene. Advanced Materials. 2019;31(18):1900509.
7. Guan Q, Zhang J, He L, Miao R, Shi Y, Ning P. Selective Hydrogenation of Acetylene to Ethylene over the Surface of Sub-2 nm Pd Nanoparticles in Miscanthus sinensis-Derived Microporous Carbon Tubes. ACS Sustainable Chemistry & Engineering. 2020;8(31):11638-11648.
8. Liu X, Mou C-Y, Lee S, Li Y, Secret J, Jang BWL. Room temperature O<sub>2</sub> plasma treatment of SiO<sub>2</sub> supported Au catalysts for selective hydrogenation of acetylene in the presence of large excess of ethylene. Journal of Catalysis. 2012;285(1):152-159.
9. Tavasoli A, Sadagiani K, Khorashe F, Seifkordi AA, Rohani AA, Nakhaeipour A. Cobalt supported on carbon nanotubes — A promising novel Fischer–Tropsch synthesis catalyst. Fuel Processing Technology. 2008;89(5):491-498.
10. Bessell S. Support effects in cobalt-based fischer-tropsch catalysis. Applied Catalysis A: General. 1993;96(2):253-268.
11. Zhang J, Chen J, Ren J, Li Y, Sun Y. Support effect of Co/Al<sub>2</sub>O<sub>3</sub> catalysts for Fischer–Tropsch synthesis. Fuel. 2003;82(5):581-586.
12. Ruta M, Semagina N, Kiwi-Minsker L. Monodispersed Pd Nanoparticles for Acetylene Selective Hydrogenation: Particle Size and Support Effects. The Journal of Physical Chemistry C. 2008;112(35):13635-13641.
13. Huang X, Yan H, Huang L, Zhang X, Lin Y, Li J, et al. Toward Understanding of the Support Effect on Pd1 Single-Atom-Catalyzed Hydrogenation Reactions. The Journal of Physical Chemistry C. 2018;123(13):7922-7930.
14. Huang X, Xia Y, Cao Y, Zheng X, Pan H, Zhu J, et al. Enhancing both selectivity and coking-resistance of a single-atom Pd1/C<sub>3</sub>N<sub>4</sub> catalyst for acetylene hydrogenation. Nano Research.



- 2017;10(4):1302-1312.
15. Yin Y, Yang Z-F, Wen Z-H, Yuan A-H, Liu X-Q, Zhang Z-Z, et al. Modification of as Synthesized SBA-15 with Pt nanoparticles: Nanoconfinement Effects Give a Boost for Hydrogen Storage at Room Temperature. *Sci Rep.* 2017;7(1):4509-4509.
  16. Al-Ammar AS, Webb G. Hydrogenation of acetylene over supported metal catalysts. Part 1.—Adsorption of [14C] acetylene and [14C]ethylene on silica supported rhodium, iridium and palladium and alumina supported palladium. *Journal of the Chemical Society, Faraday Transactions 1: Physical Chemistry in Condensed Phases.* 1978;74(0):195.
  17. Machado BF, Serp P. Graphene-based materials for catalysis. *Catal Sci Technol.* 2012;2(1):54-75.
  18. Singh V, Joung D, Zhai L, Das S, Khondaker SI, Seal S. Graphene based materials: Past, present and future. *Progress in Materials Science.* 2011;56(8):1178-1271.
  19. Tabrizi NS, Xu Q, van der Pers NM, Lafont U, Schmidt-Ott A. Synthesis of mixed metallic nanoparticles by spark discharge. *Journal of Nanoparticle Research.* 2008;11(5):1209-1218.
  20. Zhao Z, Dai Y, Lin J, Wang G. Highly-Ordered Mesoporous Carbon Nitride with Ultrahigh Surface Area and Pore Volume as a Superior Dehydrogenation Catalyst. *Chemistry of Materials.* 2014;26(10):3151-3161.
  21. Zheng Y, Jiao Y, Jaroniec M, Jin Y, Qiao SZ. Nanostructured Metal-Free Electrochemical Catalysts for Highly Efficient Oxygen Reduction. *Small.* 2012;8(23):3550-3566.
  22. Zhang Y, Mori T, Ye J, Antonietti M. Phosphorus-Doped Carbon Nitride Solid: Enhanced Electrical Conductivity and Photocurrent Generation. *Journal of the American Chemical Society.* 2010;132(18):6294-6295.
  23. Liu G, Niu P, Sun C, Smith SC, Chen Z, Lu GQ, et al. Unique Electronic Structure Induced High Photoreactivity of Sulfur-Doped Graphitic C<sub>3</sub>N<sub>4</sub>. *Journal of the American Chemical Society.* 2010;132(33):11642-11648.
  24. Xu J, Zhang L, Shi R, Zhu Y. Chemical exfoliation of graphitic carbon nitride for efficient heterogeneous photocatalysis. *Journal of Materials Chemistry A.* 2013;1(46):14766.
  25. Lakhi KS, Park D-H, Al-Bahily K, Cha W, Viswanathan B, Choy J-H, et al. Correction: Mesoporous carbon nitrides: synthesis, functionalization, and applications. *Chemical Society Reviews.* 2017;46(2):560-560.
  26. Shin EW, Kang JH, Kim WJ, Park JD, Moon SH. Performance of Si-modified Pd catalyst in acetylene hydrogenation: the origin of the ethylene selectivity improvement. *Applied Catalysis A: General.* 2002;223(1-2):161-172.
  27. Bazzazadegan H, Kazemini M, Rashidi AM. A high performance multi-walled carbon nanotube-supported palladium catalyst in selective hydrogenation of acetylene-ethylene mixtures. *Applied Catalysis A: General.* 2011;399(1-2):184-190.
  28. Patent report. *Zeolites.* 1994;14(8):701-705.
  29. Bond G, Wells P. The hydrogenation of acetylene III. The reaction of acetylene with hydrogen catalyzed by alumina-supported rhodium and iridium. *Journal of Catalysis.* 1966;5(3):419-427.
  30. Bos ANR, Westerterp KR. Mechanism and kinetics of the selective hydrogenation of ethyne and ethene. *Chemical Engineering and Processing: Process Intensification.* 1993;32(1):1-7.
  31. Vannic MA. *Handbook of Heterogeneous Catalysis.* Herausgegeben von G. Ertl, H. Knözinger und J. Weitkamp, WILEY-VCH, Weinheim, 1997. 2500 S., geb., 24900.00 DM-ISBN 3-527-29212-8. *Angewandte Chemie.* 1997;109(23):2808-2810.
  32. The Patent Agency Business. *Scientific American.* 1859;14(32):262-262.
  33. Borodziński A, Bond GC. Selective Hydrogenation of Ethyne in Ethene-Rich Streams on Palladium Catalysts. Part 1. Effect of Changes to the Catalyst During Reaction. *Catalysis Reviews.* 2006;48(2):91-144.
  34. Kim W. Deactivation behavior of a TiO<sub>2</sub>-added Pd catalyst in acetylene hydrogenation. *Journal of Catalysis.* 2004;226(1):226-229.
  35. Praserttham P, Ngamsom B, Bogdanchikova N, Phatanasri S, Pramothana M. Effect of the pretreatment with oxygen and/or oxygen-containing compounds on the catalytic performance of Pd-Ag/Al<sub>2</sub>O<sub>3</sub> for acetylene hydrogenation. *Applied Catalysis A: General.* 2002;230(1-2):41-51.
  36. Zhang Q, Li J, Liu X, Zhu Q. Synergetic effect of Pd and Ag dispersed on Al<sub>2</sub>O<sub>3</sub> in the selective hydrogenation of acetylene. *Applied Catalysis A: General.* 2000;197(2):221-228.
  37. Kang JH, Shin EW, Kim WJ, Park JD, Moon SH. Selective hydrogenation of acetylene on Pd/SiO<sub>2</sub> catalysts promoted with Ti, Nb and Ce oxides. *Catalysis Today.* 2000;63(2-4):183-188.
  38. Kang JH, Shin EW, Kim WJ, Park JD, Moon SH. Selective Hydrogenation of Acetylene on TiO<sub>2</sub>-Added Pd Catalysts. *Journal of Catalysis.* 2002;208(2):310-320.
  39. Wongwananon N, Mekasuwandumrong O, Praserttham P, Panpranot J. Performance of Pd catalysts supported on nanocrystalline  $\alpha$ -Al<sub>2</sub>O<sub>3</sub> and Ni-modified  $\alpha$ -Al<sub>2</sub>O<sub>3</sub> in selective hydrogenation of acetylene. *Catalysis Today.* 2008;131(1-4):553-558.
  40. Mei D, Sheth P, Neurock M, Smith C. First-principles-based kinetic Monte Carlo simulation of the selective hydrogenation of acetylene over Pd(111). *Journal of Catalysis.* 2006;242(1):1-15.
  41. Osswald J, Kovnir K, Armbruster M, Giedigkeit R, Jentoft R, Wild U, et al. Palladium-gallium intermetallic compounds for the selective hydrogenation of acetylene Part II: Surface characterization and catalytic performance. *Journal of Catalysis.* 2008;258(1):219-227.